Published online December 13, 2005

Nucleic Acids Research, 2005, Vol. 33, No. 22 ***e190***
doi:10.1093/nar/gni188

Quantum dots to monitor RNAi delivery and improve gene silencing

Alice A. Chen[1], Austin M. Derfus[2], Salman R. Khetani[1,2] and Sangeeta N. Bhatia[1,2,3,*]

[1]Harvard-M.I.T. Division of Health Sciences and Technology/Electrical Engineering and Computer Science, Massachusetts Institute of Technology, MA, USA, [2]Department of Bioengineering, University of California at San Diego, CA, USA and [3]Division of Medicine, Brigham & Women's Hospital, Boston, MA, USA

Received May 24, 2005; Revised and Accepted November 22, 2005

ABSTRACT

A critical issue in using RNA interference for identifying genotype/phenotype correlations is the uniformity of gene silencing within a cell population. Variations in transfection efficiency, delivery-induced cytotoxicity and 'off target' effects at high siRNA concentrations can confound the interpretation of functional studies. To address this problem, we have developed a novel method of monitoring siRNA delivery that combines unmodified siRNA with seminconductor quantum dots (QDs) as multi color biological probes. We co-transfected siRNA with QDs using standard transfection techniques, thereby leveraging the photostable fluorescent nanoparticles to track delivery of nucleic acid, sort cells by degree of transfection and purify homogenously-silenced subpopulations. Compared to alternative RNAi tracking methods (co-delivery of reporter plasmids and end-labeling the siRNA), QDs exhibit superior photostability and tunable optical properties for an extensive selection of non-overlapping colors. Thus this simple, modular system can be extended toward multiplexed gene knockdown studies, as demonstrated in a two color proof-of-principle study with two biological targets. When the method was applied to investigate the functional role of T-cadherin (T-cad) in cell–cell communication, a subpopulation of highly silenced cells obtained by QD labeling was required to observe significant downstream effects of gene knockdown.

INTRODUCTION

RNA interference (RNAi) has emerged as a powerful tool for studying gene function. Since the discovery of RNAi (1), the evolutionarily conserved cellular process has been exploited to determine the functions of nearly every gene in model organisms *Caenorhabditis elegans* (2,3) and *Drosophila melanogaster* (4) and a host of mammalian genes including ~23% of the sequenced human genes (5,6). If the RNAi effector sequence is potent and the siRNA delivered efficiently throughout the cell culture, remarkably specific post-transcriptional inhibition of gene expression can be achieved (7,8). However, inefficient and heterogeneous delivery of siRNA is frequently observed in cell cultures, causing variable levels of gene silencing and potentially confounding the interpretation of genotype/phenotype correlations (9–12). Without the means to address and resolve transfection variability, the utility of RNAi in eukaryotes will be limited only to mammalian cell types that have been thoroughly optimized for siRNA delivery (13).

The importance of high transfection efficiency has been spotlighted among numerous reports investigating methods to either improve RNAi delivery (14–17) or screen for efficient knockdown. In the latter case, typical strategies involve monitoring fluorescently end-modified siRNAs (18,19) or co-transfecting reporter plasmids and selecting for high transfection by fluorescence or antibiotic-resistance (20). These techniques enable one-time selection of highly transfected cells yet discard moderately-silenced cells, which may be of interest to the study. For example, varying degrees of RNAi-mediated down-regulation in the tumor suppressor gene *Trp53* have been shown to modulate expression of distinct pathological phenotypes both *in vitro* and *in vivo* (21). Moreover, rapid photobleaching of organic fluorophores and

*To whom correspondence should be addressed at Laboratory for Multiscale Regenerative Technologies, 77 Massachusetts Avenue, E19-502D, Cambridge, MA 02139, USA. Tel: +617 324 0221; Fax: +617 324 0740; Email: sbhatia@mit.edu

The authors wish it be known that, in their opinion, the first two authors should be regarded as joint First Authors

the limited selection of available reporters currently prevent RNAi tracking from being feasible in either long-term or multiplexed studies. The dyes commonly used to label siRNAs lose over half the intensity of fluorescent signal in 5–10 s (22,23). Meanwhile, fluorescent reporter plasmids, although meant to be continuously expressed by the cells, can require as long as 2 h after transcription for the functional protein to be observable (24). Perhaps most importantly, due to the limited availability of fluorophores and reporter proteins that have non-overlapping emission spectra, current transfection screening methods are incapable of simultaneous monitoring of multiple siRNA molecules.

In this study, we demonstrate a novel means of monitoring nucleic acid delivery using standard transfection techniques to co-deliver semiconductor quantum dots (QDs) along with siRNA. QDs are bright, photostable CdSe/ZnS fluorescent nanocrystals that exhibit tunable emission properties for a wide range of color possibilities. We and others have shown that QDs can be rendered non-cytotoxic (25) and innocuous to normal cell physiology and common cellular assays, such as immunostaining and reporter gene expression (26). Combining QDs with siRNA for RNAi tracking requires neither chemical labeling of siRNA, which is costly and can potentially deter complexing with RISC, nor the expression of reporter plasmids. QDs are also brighter than most conventional fluorescent dyes by ~10-fold (22,27) and have been significantly easier to detect than green fluorescent protein (GFP) among background autofluorescence *in vivo* (27). Furthermore, QDs are far less susceptible to photobleaching, fluorescing more than 20 times longer than conventional fluorescent dyes under continuous mercury lamp exposure (28). Using our QD/siRNA co-delivery technique, we found that cellular fluorescence correlated with level of silencing, allowing collection of a uniformly silenced cell population by fluorescence-activated cell sorting (FACS). The superior brightness and photostability of these probes in cells sustained not only FACS, but also live imaging, and immunostaining procedures. With two QD colors and two siRNAs as a model, we also demonstrate the method's unique ability to generate cell populations with multiplexed levels of knockdown. Finally, we show that a homogenous silenced cell population generated using this method is essential to observe the phenotypic effects of decreased T-cadherin (T-cad) protein expression on cell–cell communication between hepatocytes and non-parenchymal cells.

MATERIALS AND METHODS

Short interfering RNA and QD preparation

Pre-designed siRNA was used to selectively silence the Lamin A/C gene (*Lmna* siRNA #73605, NM_019390, Ambion) and the T-cad gene (SMARTpool reagent CDH13, NM_019707, Dharmacon). Fluorescently-labeled *Lmna* siRNA purchased from Dharmacon was designed with a fluorescein molecule on the 5′ end of the sense strand. The annealed sequences were reconstituted in nuclease-free water and used at a concentration of 100 nM (*Lmna* siRNA, 5′-Fluorescein-*Lmna* siRNA) or 50 nM (T-cad siRNA).

Green (560 nm emission maxima) and orange (600 nm emission maxima) CdSe-core, ZnS-shell nanocrystals were synthesized and water-solubilized with mercaptoacetic acid (MAA) as described previously (29–31). MAA-QDs were then surface-modified by reacting with polyethylene glycol (PEG)-thiol MW 5000 (Nektar) overnight at room temperature. Excess PEG-thiol was removed by spin filtration (100 kDa cut-off). QDs are also available commercially as an alternative to synthesis (Quantum Dot Corp., Evident Technologies). Unless stated otherwise, 5 μg PEGylated QD was used per cell transfection.

Fibroblast cell culture and transfection

Fibroblasts (3T3-J2) were provided by Howard Green (Harvard Medical School, Cambridge, MA) (32) and cultured at 37°C, 5% CO_2 in DMEM with high glucose, 10% fetal bovine serum (FBS) and 1% penicillin–streptomycin. The transfection procedure was performed using Lipofectamine 2000 (Invitrogen) according to the manufacturer's instructions. Briefly, 3T3 fibroblasts were plated 24 h before transfection at a density of 3×10^6 cells per 35 mm well, in antibiotic- and serum-free medium. Lipofectamine reagent (5 μl) and either siRNA or QDs were diluted in DMEM and complexed at room temperature. For QD/siRNA co-complexes, siRNA and liposomes were allowed to complex for 15 min before an additional 15 min incubation with QDs. Complexes were added to cell cultures in fresh antibiotic- and serum-free medium until 5 h later, at which time the cultures were washed and replaced with regular growth medium. Approximately 24 h post-transfection, cells were trypsinized and prepared for flow cytometry.

FACS

Flow cytometry and sorting was performed on a FACS Vantage SE flow cytometer (Becton Dickinson) using a 488 nm Ar laser and FL1 bandpass emission (530 ± 20 nm) for the green QDs, FL3 bandpass emission (610 ± 10 nm) for the orange QDs. Fluorescence histograms and dot plots were generated using Cell Quest software (for figures, histograms were re-created using WinMDI software, http://facs.scripps.edu). Cell Quest was also used to gate populations of highest and lowest fluorescence intensity for sorting into chilled FBS. Sorted populations were immediately re-plated into separate wells containing regular growth medium and allowed to adhere. Cells were incubated at 37°C until visualized by fluorescence microscopy or until assayed for protein level.

Western blotting

Cell cultures were scraped and lysed in RIPA Lysis Buffer (Upstate Biotechnologies) supplemented with COMPLETE EDTA-free Protease inhibitor solution (Roche). Equal amounts (15–20 μg) of total protein were loaded into 10% Tris–HCl resolving gel, separated by electrophoresis and transferred to PVDF membrane. The blot was incubated in blocking solution (5% [w/v] non-fat dry milk, 200 mM Tris base (pH 7.4), 5 M NaCl and 5% Tween-20) for 1 h at room temperature, primary antibody overnight at 4°C, and secondary antibody for 1 h. Three washes in 200 mM Tris base (pH 7.4), 5 M NaCl and 5% Tween-20 took place between steps and after completion of probing. Finally, the blot was visualized by chemiluminscence (Super Signal West Pico Kit, Pierce) and developed. Bands were analyzed for density using

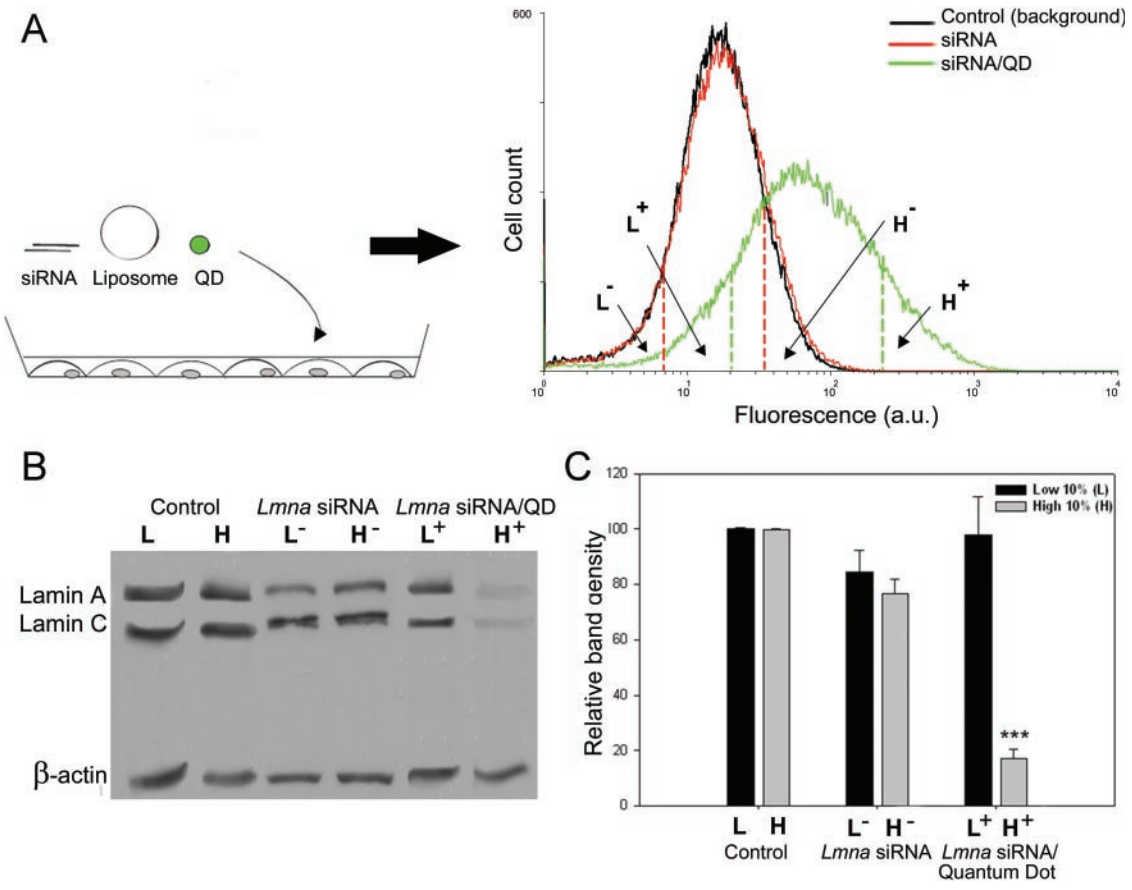

Figure 1. QD/siRNA complexes allow sorting of gene silencing in cell populations. (**A**) Schematic representation of cells co-transfected with QDs and siRNA and analyzed for intracellular fluorescence by flow cytometry. Histograms depict fluorescence distributions of control murine fibroblast cells, *Lmna* siRNA-treated cells and *Lmna* siRNA/QD-treated cells. FACS was used to gate and sort the high 10% (H) fluorescence and low 10% (L) fluorescence of each distribution. L^- and H^- point to gates for the siRNA only histogram. L^+ and H^+ indicate gates for the siRNA/QD histogram. (**B**) Representative western blot of Lamin A/C protein expression levels in sorted cells with β-actin as loading control. Control lanes are protein from cells mock-transfected with liposome reagent only and sorted (L and H). The absence of QDs is indicated by a minus sign (−) and the presence of QDs is indicate by a plus sign (+). (**C**) Band densitometry analysis of western blots from replicate experiments. Error bars represent standard error of the mean ($n = 3$). ***$P < 0.001$ (One-way ANOVA).

MetaMorph Image Analysis software (Universal Imaging) and normalized to loading control (β-actin) bands.

Primary antibodies used were polyclonal lamin A/C antibody (Cell Signaling) at 1:1000 dilution in blocking solution and polyclonal β-actin antibody (Cell Signaling) at 1:750 dilution. T-cad primary antibody was a gift from Barbara Ranscht (University of California, San Diego) (33). Secondary antibody was goat anti-rabbit IgG-horseradish peroxidase (HRP) (Santa Cruz Biotechnology) at 1:7500 dilution. Blots were probed simultaneously for lamin A/C protein (70 kDa and 28 kDa) and β-actin protein (45 kDa); after detection, select blots were re-probed for T-cad (95 kDa).

Immunofluorescence staining

Sorted and unsorted cells intended for lamin nuclear protein immunostaining were seeded on to Collagen-I coated glass coverslips. Coverslips with attached cells were washed twice in cold phosphate-buffered saline (PBS, Gibco) and fixed in 4% paraformaldehyde at room temperature. After three brief PBS washes, cells were permeabilized with 0.2% Triton X for 10 min at room temperature and washed again. The cells were blocked with 10% goat serum for 30 min at 37°C, incubated in primary antibody (1:100 Lamin A antibody, Santa Cruz Biotechnology) for 90 min at 37°C, washed three times with 0.05% Triton X, incubated in secondary antibody (1:250 AlexaFluor 594 chicken anti-rabbit IgG antibody, Molecular Probes) for 1 h at room temperature, and washed a final three times. Antibody dilutions were performed in 1% BSA in PBS. Coverslips were mounted on to glass slides using Vectashield anti-fade medium (Vector Laboratories). Finally, nuclear staining was visualized and documented by phase contrast microscopy or epifluorescence (Nikon Ellipse TE200 inverted fluorescence microscope and CoolSnap-HQ Digital CCD Camera).

Hepatocyte/fibroblast co-cultures

Hepatocytes were isolated from 2 to 3 month old adult female Lewis rats (Charles River Laboratories) and purified as described previously (34,35). Fresh, isolated hepatocytes were seeded at a density of 2.5×10^5 cells per well, in 17 mm wells adsorbed with 0.13 mg/ml Collagen-I. Cultures were maintained at 37°C, 5% CO_2 in hepatocyte medium consisting of DMEM with high glucose, 10% FBS, 0.5 U/ml insulin, 7 ng/ml glucagons, 7.5 μg/ml hydrocortisone, 10 U/ml

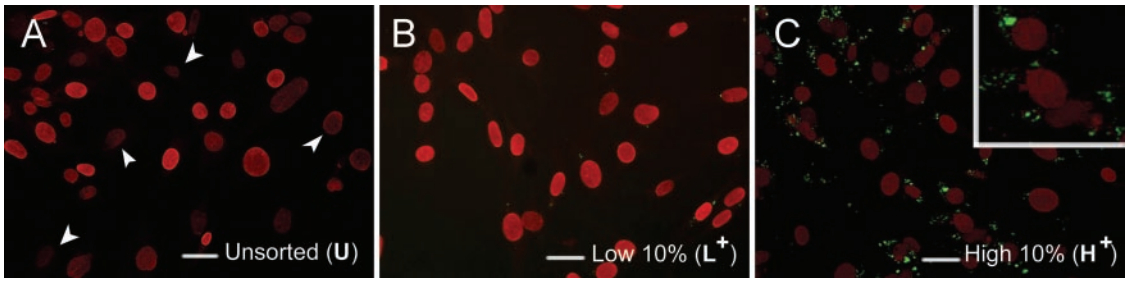

Figure 2. Immunofluorescence staining of Lamin A/C nuclear protein (red). (**A**) Unsorted cells (U) transfected with *Lmna* siRNA alone display heterogenous staining for nuclear lamin throughout the cell population. White arrows highlight examples of cells with weak lamin staining among cells stained strongly for lamin. (**B**) Cells co-transfected with *Lmna* siRNA and green QDs exhibit bright lamin staining and lack of QDs in low-gated (L^+) cell subpopulations and (**C**) weak lamin staining and presence of QDs in high-gated (H^+) cell subpopulations (shown enlarged in inset). Scale bars 75 μm.

penicillin and 10 μg/ml streptomycin. After 24 h of hepatocyte seeding, the fibroblasts from transfection experiments were co-cultivated at a previously optimized 1:1 hepatocyte:fibroblast ratio in fibroblast medium (36). Medium from hepatocyte/fibroblast co-cultures was collected and replaced with hepatocyte medium every 24 h until completion of the experiment.

Hepatocellular function assays

Hepatocyte/fibroblast co-cultures were assayed for albumin production and cytochrome P450 enzymatic activity, prototypic indicators of hepatocellular function (37,38). Albumin content in spent media samples was measured using an enzyme linked immunosorbent assay (ELISA) with HRP detection (35). Cytochrome P450 (CYP1A1) enzymatic activity was measured by quantifying the amount of resorufin produced from the CYP-mediated cleavage of ethoxyresorufin *O*-deethylase (EROD) (39). Specifically, EROD was incubated with cell cultures for 30 min, media was collected and resorufin fluorescence quantified at 571/585 nm excitation/emission.

Error bars represent standard error of the mean ($n = 3$). Statistical significance was determined using one-way ANOVA.

RESULTS AND DISCUSSION

We used cationic liposomes to co-deliver green QDs and siRNA targeting the lamin a/c gene (*Lmna*) into murine fibroblasts, followed by flow cytometry to quantify intracellular QD uptake (Figure 1A). The median fluorescence of QD/siRNA-transfected cells compared to mock-transfected cells (liposome reagent only) and cells transfected with siRNA alone varied by ~84% (coefficient of variation). FACS was used to gate and collect the brightest 10% (high, H) of each fluorescence distribution, along with the dimmest 10% (low, L). After the sorted cells were re-plated and grown for 72 h to ensure protein turnover, protein expression analysis by either western blot or immunostaining was performed. In cells that had been co-transfected with siRNA and QDs, gene silencing correlated directly with intracellular fluorescence. Western blotting (Figure 1B) and image analysis of lamin a/c protein bands (Figure 1C) show ~90% knockdown in the highly fluorescent cells and negligible knockdown in the dimmest cells. The cells treated with siRNA alone exhibited mediocre gene down-regulation (20–30%) independent of sorting parameters.

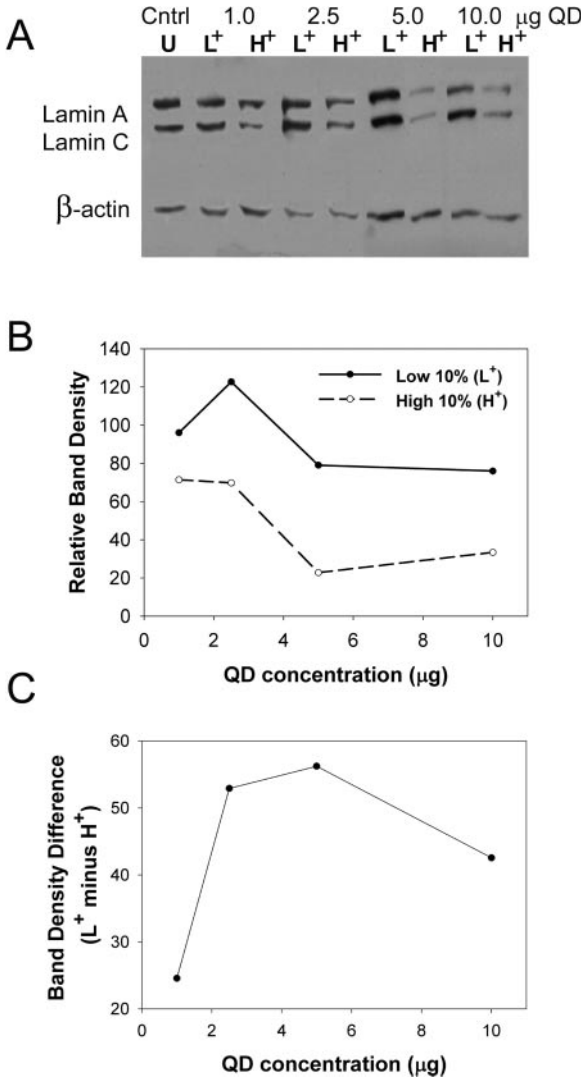

Figure 3. Optimization of QD concentration for siRNA tracking. *Lmna* siRNA (100 nM) and 1, 2.5, 5 or 10 μg QD were co-transfected into murine fibroblasts and the cells FACS-sorted for the low 10% (L^+) and high 10% (H^+) of intracellular fluorescence distribution. (**A**) Protein expression of sorted cells assayed by western blot, β-actin loading control. Unsorted, lipofectamine only control (U) represented 100% lamin a/c protein expression. (**B**) Western blot band densitometry analysis of L^+ and H^+ bands shows an optimum QD concentration for obtaining high-efficiency silencing. (**C**) Band density difference (L^+ minus H^+) reveals an optimum QD concentration for sorting most efficiently silenced from least efficiently silenced subpopulations.

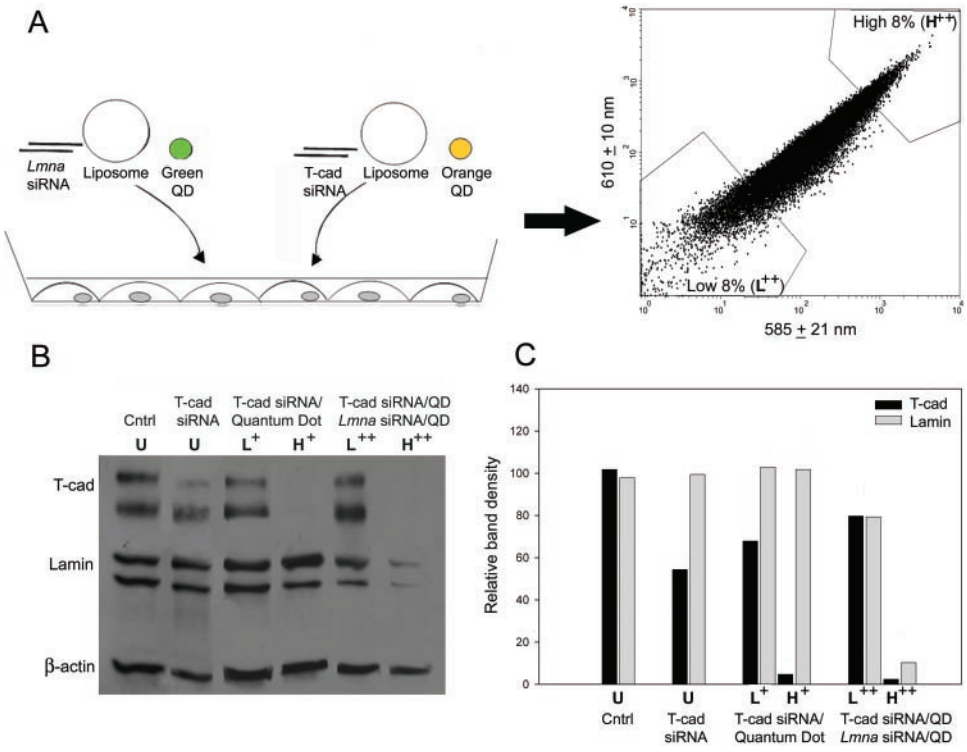

Figure 4. Sorting the effects of double gene knockdowns using two colors of QDs. (**A**) Schematic representation of cells transfected simultaneously with *Lmna* siRNA/green QD complexes and T-cad siRNA/orange QD complexes. The low 8% (L^{++}, where ++ designates the presence of two colors of QDs) and high 8% (H^{++}) of the dual fluorescence dot plot was gated and isolated using FACS. (**B**) Representative western blot and (**C**) corresponding band densitometry analysis of lamin A/C and T-cad protein levels in control unsorted (U) cells, unsorted (U) T-cad siRNA-treated cells, sorted T-cad/QD-treated cells (L^{+} and H^{+}) and sorted dual siRNA/dual QD-treated (L^{++} and H^{++}) cells.

Consistent with the quantitative bulk protein assay, immunofluorescent detection of lamin nuclear protein in unsorted, siRNA-transfected cells produced heterogeneous staining throughout the cell population (Figure 2A). However, in the co-transfected case, the presence of green QDs correlated with consistently weak lamin immunofluorescent staining in the high co-transfected subpopulation (Figure 2B), compared to a lack of observable QDs and strong lamin staining in the low subpopulation (Figure 2C). Heterogeneous silencing therefore influences the accuracy of the bulk protein expression readout, suggesting the importance of verifying successful siRNA transfection for each gene knockdown study. Using QDs as photostable probes in combination with FACS, a subpopulation of uniformly-treated cells can be isolated, and also tracked with fluorescence microscopy over long periods of time. This may be useful for observing the protein down-regulation and phenotypic responses of cells to gene regulation over time.

To optimize the QD/siRNA correlative effect, we varied the ratio of QD to lipofection reagent with a fixed dose of 100 nM siRNA. Specifically, we co-complexed *Lmna* siRNA with QD:lipofection reagent ratios of 1:5, 1:2, 1:1 or 2:1 (corresponding to 1, 2.5, 5 or 10 μg QD) and sorted the high 10% and low 10% of the cell fluorescence distributions as before. We found that optimal fluorescence and gene silencing correlation for the least amount of QD occurs at a 1:1 QD:lipofection reagent mass ratio (5 μg QD), as assayed by western blot (Figure 3A–C). We hypothesize that this optimum results from the limited surface area of the cationic liposome delivery agent (~1 μm^2) that is shared by the siRNA and QDs during the complexing process. Using too few QDs fails to provide fluorescence that is detectable over background, whereas excess QDs occupy sites on the liposome that would otherwise be available to siRNA. In support of this theory, we found that saturating the liposome with QDs (100:1 ratio) before transfection abolished correlation between cellular fluorescence and gene silencing; both high- and low-populations exhibited little to no knockdown (data not shown).

QDs exhibit an extensive range of size- and composition-dependent optical properties, making them uniquely advantageous for multiplexing i.e. monitoring and sorting cells that have been treated simultaneously with different siRNA/QD complexes. As a proof-of-principle, we complexed cationic liposomes with either green (em 560 nm) QDs and *Lmna* siRNA or orange (em 600 nm) QDs and siRNA targeting T-cad. Cells were exposed simultaneously to both complexes and flow cytometry was used to quantify orange fluorescence (600 ± 10 nm) versus green fluorescence (560 ± 20 nm) (Figure 4A). Cells exhibiting dual color fluorescence were gated for low 8% and high 8% fluorescence and collected. Western blots probing lamin a/c and T-cad protein confirm specificity of QD/siRNA complexing (Figure 4B and C), while fluorescence microscopy validates gating accuracy and demonstrates multi color tracking capabilities (Figure 5). Unsorted cells transfected with T-cad siRNA alone expressed a 45% down-regulation in protein expression quantified by Western blot band densitometry. In contrast, co-delivery of QDs with T-cad siRNA and subsequent sorting enabled separation of the least efficiently transfected cell subpopulation

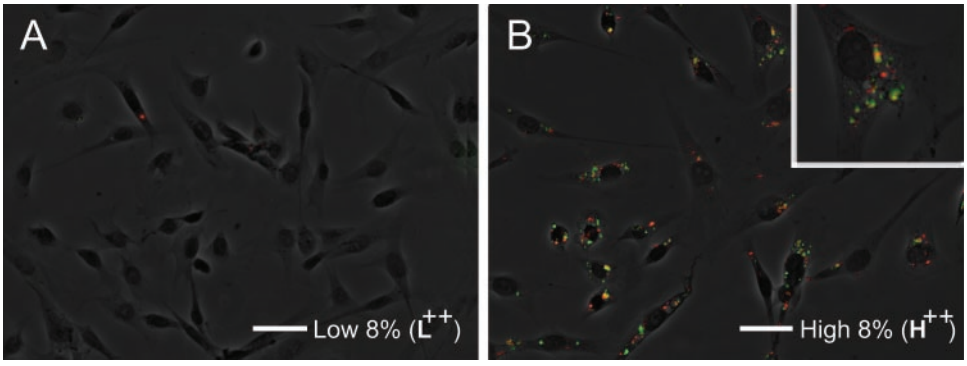

Figure 5. Fluorescence/phase micrographs of two color QD transfections. (**A**) Low-gated cells (L^{++}, where ++ indicates the presence of two colors of QD) nearly lack orange or green QDs. (**B**) High-gated cells (H^{++}) fluoresce brightly with punctate green and orange QDs (enlarged in inset). Scale bars 100 μm.

(30% protein knockdown) from a highly transfected population (95% knockdown). In the highest 8% of the dual color, dual siRNA co-transfected cell population, highly effective silencing of both *Lmna* gene (96% knockdown) and T-cad gene (98% knockdown) was achieved. Given the wide spectrum of QD color possibilities, this method promises to be useful for tracking and sorting multiple siRNA-mediated knockdowns within one cell population.

The utility of RNAi as a functional genomics tool is predicated upon associating gene silencing with downstream phenotypic observations. Yet non-uniform gene silencing may obscure bulk measurements (protein and mRNA) commonly used to validate gene knockdown and obscure genotype/phenotype correlations. We compared the downstream effects of non-uniform and homogenous gene silencing to specifically examine the stabilizing effect of non-parenchymal cells (3T3 fibroblasts) on hepatocellular function *in vitro* (36). Recently, several cadherins from hepatocyte-fibroblast junctions were identified as potential mediators of liver-specific function *in vitro* (37). Based on this finding, we transfected fibroblasts with T-cad siRNA or T-cad siRNA/QD complexes, sorted each population according to high or low cellular fluorescence, and co-cultivated the populations with hepatocytes. Markers of liver-specific function, albumin synthesis and cytochrome P450 1A1 (CYP1A1) activity, were measured in hepatocyte/3T3 co-cultures (Figure 6). Compared to control co-cultures, significant down-regulation in hepatocellular function (2-fold) was observed exclusively in the cultures that had been treated with T-cad siRNA/QD complexes and sorted for high cellular fluorescence. These studies implicate a role for fibroblast T-cad protein expression in modulating hepatocellular function *in vitro*, an interpretation revealed only once a homogenously-silenced population of fibroblasts was obtained.

In this work, we have identified a role for T-cad in cell–cell communication between hepatocytes and non-parenchymal cells using a technically simple method for enriching transfected cells which can be applied to further studies. Attempts to improve silencing by simply using higher concentrations of siRNA do not improve knockdown but may actually negatively regulate RNAi-mediated gene silencing (Supplementary Figure S1) (40,41). In addition, excesses of either siRNA or cationic liposome has been shown to induce increased cytotoxicity, interferon response (42) and 'off-target' effects (43). While current techniques are available to fluorescently track

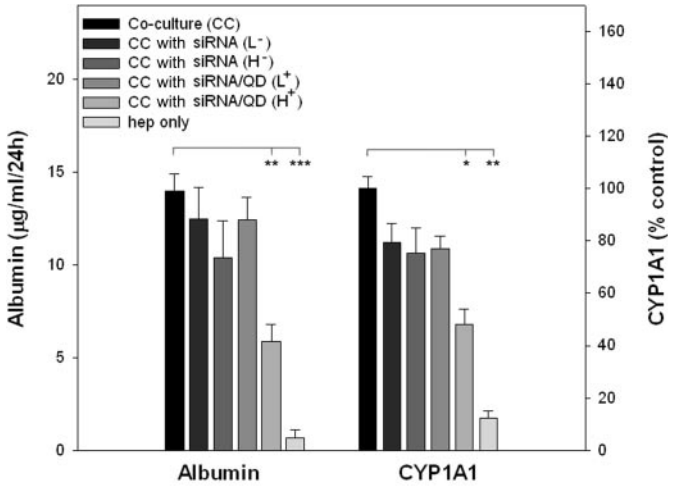

Figure 6. Significant downstream gene knockdown effects of T-cad gene silencing are observed only in a homogenous silenced cell population. Murine 3T3 fibroblasts transfected with T-cad siRNA alone or with T-cad siRNA/QD complexes were FACS-sorted for low 10% (L) or high 10% (H) intracellular fluorescence. Symbols − and + indicate the absence or presence of QD during transfection. To study the stabilizing effect of non-parenchymal cell (3T3 fibroblast) protein expression on liver-specific function, control or transfected/sorted 3T3 cells were added to hepatocyte cultures 24 h after hepatocyte seeding. Liver-specific function was assayed by measuring albumin synthesis and cytochrome P450 1A1 (CYP1A1) activity of cultured media sampled at 72 and 96 h after 3T3 seeding and averaged. Error bars represent standard error of the mean ($n = 3$). $^{*}P < 0.05$, $^{**}P < 0.01$, $^{***}P < 0.001$ (One-way ANOVA statistical analysis test).

RNAi delivery (co-delivery of fluorescent protein expressing plasmids, end-labeling with a dye), none offer such a simple, modular and versatile means to generate a homogeneously silenced population. In addition to superiority over dyes in brightness and photostability (Supplementary Figure S2), multi color QD labels can be used interchangeably, with all particle sizes employing a common, passive mechanism to form delivery complexes. The point at which a cell's RNAi machinery saturates is not yet known; yet at the least this capability simplifies known strategies to enrich for dual gene knockdowns using antibiotic-resistant markers that are co-transfected, transcribed and selected. The numerous non-overlapping color possibilities of QDs (12 commercially available in the spectral range of FACS detectors) may further enable multiplexed and combinatorial gene studies for the

potential illumination of entire biological pathways. Use of commercial QDs in the amounts specified would be reasonably economical- approximately the same cost as the liposome reagent and approximately four times lower than the synthesis of dye-labeled RNA. As shown in previous work, QDs are compatible with a variety of transfection techniques (other reagents, electroporation and microinjection) and therefore amenable to nucleic acid monitoring in cells that are susceptible to liposome-triggered cytotoxicity (44). Primary cells may be particularly suited to benefit from this method, as non-viral delivery of siRNA has to date been technically difficult. Thus, ODs are versatile, photostable probes that offer an added dimension to improve the power of RNAi as an experimental tool.

SUPPLEMENTARY DATA

Supplementary Data are available at NAR Online.

ACKNOWLEDGEMENTS

We thank Mike Sailor for providing facilities for QD synthesis, Dennis Young for his assistance with flow cytometry, Barbara Ranscht for providing antibody, Jennifer Felix and Kathryn Hudson for hepatocyte isolation, Howard Green for supplying 3T3-J2 fibroblasts and Lee Gehrke for comments on the manuscript. Funding was generously provided by the National Science Foundation (A.A.C.), a G.R.E.A.T. fellowship from UC-BREP (2004-16) (A.M.D.), the David and Lucille Packard Foundation, NIH NIDDK (#R01 DK065152, #R01 DK56966), NIH NCI (#N01 CO37117) and NASA. Funding to pay the Open Access publication charges for this article was provided by NIH NCI (#U54 CA119349).

Conflict of interest statement. None declared.

REFERENCES

1. Fire,A., Xu,S., Montgomery,M.K., Kostas,S.A., Driver,S.E. and Mello,C.C. (1998) Potent and specific genetic interference by double-stranded RNA in *Caenorhabditis elegans*. *Nature*, **391**, 806–811.
2. Kamath,R.S., Fraser,A.G., Dong,Y., Poulin,G., Durbin,R., Gotta,M., Kanapin,A., Le Bot,N., Moreno,S., Sohrmann,M. *et al*. (2003) Systematic functional analysis of the *Caenorhabditis elegans* genome using RNAi. *Nature*, **421**, 231–237.
3. Maeda,I., Kohara,Y., Yamamoto,M. and Sugimoto,A. (2001) Large-scale analysis of gene function in *Caenorhabditis elegans* by high-throughput RNAi. *Curr. Biol.*, **11**, 171–176.
4. Boutros,M., Kiger,A.A., Armknecht,S., Kerr,K., Hild,M., Koch,B., Haas,S.A., Consortium,H.F., Paro,R. and Perrimon,N. (2004) Genome-wide RNAi analysis of growth and viability in *Drosophila* cells. *Science*, **303**, 832–835.
5. Zheng,L., Liu,J., Batalov,S., Zhou,D., Orth,A., Ding,S. and Schultz,P.G. (2004) An approach to genomewide screens of expressed small interfering RNAs in mammalian cells. *Proc. Natl Acad. Sci. USA*, **101**, 135–140.
6. Novina,C.D. and Sharp,P.A. (2004) The RNAi revolution. *Nature*, **430**, 161–164.
7. Chi,J.T., Chang,H.Y., Wang,N.N., Chang,D.S., Dunphy,N. and Brown,P.O. (2003) Genomewide view of gene silencing by small interfering RNAs. *Proc. Natl Acad. Sci. USA*, **100**, 6343–6346.
8. Semizarov,D., Frost,L., Sarthy,A., Kroeger,P., Halbert,D.N. and Fesik,S.W. (2003) Specificity of short interfering RNA determined through gene expression signatures. *Proc. Natl Acad. Sci. USA*, **100**, 6347–6352.
9. Raab,R.M. and Stephanopoulos,G. (2004) Dynamics of gene silencing by RNA interference. *Biotechnol. Bioeng.*, **88**, 121–132.
10. Huppi,K., Martin,S.E. and Caplen,N.J. (2005) Defining and assaying RNAi in mammalian cells. *Mol. Cell*, **17**, 1–10.
11. Spagnou,S., Miller,A.D. and Keller,M. (2004) Lipidic carriers of siRNA: differences in the formulation, cellular uptake, and delivery with plasmid DNA. *Biochemistry*, **43**, 13348–13356.
12. Oberdoerffer,P., Kanellopoulou,C., Heissmeyer,V., Paeper,C., Borowski,C., Aifantis,I., Rao,A. and Rajewsky,K. (2005) Efficiency of RNA interference in the mouse hematopoietic system varies between cell types and developmental stages. *Mol. Cell Biol.*, **25**, 3896–3905.
13. McManus,M.T. and Sharp,P.A. (2002) Gene silencing in mammals by small interfering RNAs. *Nature Rev. Genet.*, **3**, 737–747.
14. Muratovska,A. and Eccles,M.R. (2004) Conjugate for efficient delivery of short interfering RNA (siRNA) into mammalian cells. *FEBS Lett.*, **558**, 63–68.
15. Lorenz,C., Hadwiger,P., John,M., Vornlocher,H.P. and Unverzagt,C. (2004) Steroid and lipid conjugates of siRNAs to enhance cellular uptake and gene silencing in liver cells. *Bioorg. Med. Chem. Lett.*, **14**, 4975–4977.
16. Schiffelers,R.M., Ansari,A., Xu,J., Zhou,Q., Tang,Q., Storm,G., Molema,G., Lu,P.Y., Scaria,P.V. and Woodle,M.C. (2004) Cancer siRNA therapy by tumor selective delivery with ligand-targeted sterically stabilized nanoparticle. *Nucleic Acids Res.*, **32**, e149.
17. Itaka,K., Kanayama,N., Nishiyama,N., Jang,W.D., Yamasaki,Y., Nakamura,K., Kawaguchi,H. and Kataoka,K. (2004) Supramolecular nanocarrier of siRNA from PEG-based block catiomer carrying diamine side chain with distinctive pKa directed to enhance intracellular gene silencing. *J. Am. Chem. Soc.*, **126**, 13612–13613.
18. Manoharan,M. (2004) RNA interference and chemically modified small interfering RNAs. *Curr. Opin. Chem. Biol.*, **8**, 570–579.
19. Chiu,Y.L., Ali,A., Chu,C.Y., Cao,H. and Rana,T.M. (2004) Visualizing a correlation between siRNA localization, cellular uptake, and RNAi in living cells. *Chem. Biol.*, **11**, 1165–1175.
20. Kumar,R., Conklin,D.S. and Mittal,V. (2003) High-throughput selection of effective RNAi probes for gene silencing. *Genome Res.*, **13**, 2333–2340.
21. Hemann,M.T., Fridman,J.S., Zilfou,J.T., Hernando,E., Paddison,P.J., Cordon-Cardo,C., Hannon,G.J. and Lowe,S.W. (2003) An epi-allelic series of p53 hypomorphs created by stable RNAi produces distinct tumor phenotypes *in vivo*. *Nature Genet.*, **33**, 396–400.
22. Wu,X., Liu,H., Liu,J., Haley,K.N., Treadway,J.A., Larson,J.P., Ge,N., Peale,F. and Bruchez,M.P. (2003) Immunofluorescent labeling of cancer marker Her2 and other cellular targets with semiconductor quantum dots. *Nat. Biotechnol.*, **21**, 41–46.
23. Dahan,M., Levi,S., Luccardini,C., Rostaing,P., Riveau,B. and Triller,A. (2003) Diffusion dynamics of glycine receptors revealed by single-quantum dot tracking. *Science*, **302**, 442–445.
24. Tsien,R.Y. (1998) The green fluorescent protein. *Annu. Rev. Biochem.*, **67**, 509–544.
25. Derfus,A.M., Chan,W.C. and Bhatia,S. (2004) Probing the cytotoxicity of semiconductor quantum dots. *Nano Lett.*, **4**, 11–18.
26. Mattheakis,L.C., Dias,J.M., Choi,Y.J., Gong,J., Bruchez,M.P., Liu,J. and Wang,E. (2004) Optical coding of mammalian cells using semiconductor quantum dots. *Anal. Biochem.*, **327**, 200–208.
27. Gao,X., Cui,Y., Levenson,R.M., Chung,L.W. and Nie,S. (2004) *In vivo* cancer targeting and imaging with semiconductor quantum dots. *Nat. Biotechnol.*, **22**, 969–976.
28. Derfus,A.M., Chan,W.C.W. and Bhatia,S.N. (2004) Intracellular Delivery of Quantum Dots for Live Cell Labeling and Organelle Tracking. *Adv. Mater.*, **16**, 961–966.
29. Chan,W.C. and Nie,S. (1998) Quantum dot bioconjugates for ultrasensitive nonisotopic detection. *Science*, **281**, 2016–2018.
30. Hines,M.A. and Guyot-Sionnest,P. (1996) Synthesis and characterization of strongly luminescing ZnS-Capped CdSe nanocrystals. *J. Phys. Chem.*, **100**, 468–471.
31. Dabbousi,B.O., RodriguezViejo,J., Mikulec,F.V., Heine,J.R., Mattoussi,H., Ober,R., Jensen,K.F. and Bawendi,M.G. (1997) (CdSe)ZnS core-shell quantum dots: Synthesis and characterization of a size series of highly luminescent nanocrystallites. *J. Phys. Chem. B*, **101**, 9463–9475.
32. Rheinwald,J.G. and Green,H. (1975) Serial cultivation of strains of human epidermal keratinocytes: the formation of keratinizing colonies from single cells. *Cell*, **6**, 331–343.
33. Ranscht,B. and Dours-Zimmermann,M.T. (1991) T-cadherin, a novel cadherin cell adhesion molecule in the nervous system lacks the conserved cytoplasmic region. *Neuron*, **7**, 391–402.

34. Seglen,P.O. (1976) Preparation of isolated rat liver cells. *Methods Cell Biol.*, **13**, 29–83.
35. Dunn,J.C., Tompkins,R.G. and Yarmush,M.L. (1991) Long-term *in vitro* function of adult hepatocytes in a collagen sandwich configuration. *Biotechnol. Prog.*, **7**, 237–245.
36. Bhatia,S.N., Balis,U.J., Yarmush,M.L. and Toner,M. (1999) Effect of cell-cell interactions in preservation of cellular phenotype: cocultivation of hepatocytes and nonparenchymal cells. *FASEB J.*, **13**, 1883–1900.
37. Khetani,S., Szulgit,G., Rio,J.D., Barlow,C. and Bhatia,S.N. (2004) Exploring interactions between hepatocytes and nonparenchymal cells using gene expression profiling. *Hepatology*, **40**, 545–554.
38. Allen,J.W., Johnson,R.S. and Bhatia,S.N. (2005) Hypoxic inhibition of 3-methylcholanthrene-induced CYP1A1 expression is independent of HIF-1alpha. *Toxicol. Lett.*, **155**, 151–159.
39. Behnia,K., Bhatia,S., Jastromb,N., Balis,U., Sullivan,S., Yarmush,M. and Toner,M. (2000) Xenobiotic metabolism by cultured primary porcine hepatocytes. *Tissue Eng.*, **6**, 467–479.
40. Hong,J., Qian,Z., Shen,S., Min,T., Tan,C., Xu,J., Zhao,Y. and Huang,W. (2005) High doses of siRNAs induce eri-1 and adar-1 gene expression and reduce the efficiency of RNA interference in the mouse. *Biochem. J.*, **390**, 675–679.
41. Kennedy,S., Wang,D. and Ruvkun,G. (2004) A conserved siRNA-degrading RNase negatively regulates RNA interference in *C. elegans*. *Nature*, **427**, 645–649.
42. Sledz,C.A., Holko,M., de Veer,M.J., Silverman,R.H. and Williams,B.R. (2003) Activation of the interferon system by short-interfering RNAs. *Nature Cell Biol.*, **5**, 834–839.
43. Jackson,A.L., Bartz,S.R., Schelter,J., Kobayashi,S.V., Burchard,J., Mao,M., Li,B., Cavet,G. and Linsley,P.S. (2003) Expression profiling reveals off-target gene regulation by RNAi. *Nat. Biotechnol.*, **21**, 635–637.
44. Hirko,A., Tang,F. and Hughes,J.A. (2003) Cationic lipid vectors for plasmid DNA delivery. *Curr. Med. Chem.*, **10**, 1185–1193.